

# Designing illuminant spectral power distributions for surface classification - Supplemental Material

Henryk Blasinski, Joyce Farrell, Brian Wandell  
Department of Electrical Engineering, Stanford University  
Stanford, CA

hblasins, joyce\_farrell, wandell@stanford.edu

## Abstract

There are many scientific, medical and industrial imaging applications where users have full control of the scene illumination and color reproduction is not the primary objective. For example, it is possible to co-design sensors and spectral illumination in order to classify and detect changes in biological tissues, organic and inorganic materials, and object surface properties. In this paper, we propose two different approaches to illuminant spectrum selection for surface classification. In the first approach, a supervised framework, we formulate a biconvex optimization problem where we alternate between optimizing support vector classifier weights and optimal illuminants. In the second approach, an unsupervised dimensionality reduction, we describe and apply a new sparse Principal Component Analysis (PCA) algorithm. We efficiently solve the non-convex PCA problem using a convex relaxation and Alternating Direction Method of Multipliers (ADMM). We compare the classification accuracy of a monochrome imaging sensor with optimized illuminants to the classification accuracy of conventional RGB cameras with natural broadband illumination.

## 1. Relaxation ADMM solver

The unsupervised illuminant selection algorithm is iterative and operates on the spectral radiance covariance matrix. First, a single optimal, nonnegative projection direction is computed by solving a relaxed nonnegative sparse PCA problem using the Alternating Direction Method of Multipliers (ADMM) [1, 5]. To derive the ADMM solver it is necessary to represent the nonnegative sparse PCA problem in an equivalent form

$$\begin{aligned} & \text{minimize} && -\text{tr}(\Sigma Y_1) + \mathbf{I}_{\mathcal{F}}(Y_1) + \mathbf{I}_+(Y_2) + \alpha \|Y_2\|_1 \\ & \text{subject to} && BWB^T - Y_1 = 0, \\ & && BWB^T - Y_2 = 0, \end{aligned} \quad (1)$$

The indicator function  $\mathbf{I}_{\mathcal{F}}$ , also called a Fantope indicator, is defined as

$$\mathbf{I}_{\mathcal{F}}(Y) = \begin{cases} 0 & \text{if } 0 \preceq Y \preceq I \wedge \text{tr}(Y) = 1 \\ \infty & \text{otherwise} \end{cases} \quad (2)$$

The second function  $\mathbf{I}_+$  is an indicator function of a matrix with positive entries

$$\mathbf{I}_+(Y) = \begin{cases} 0 & y_{ij} \geq 0 \forall ij \\ \infty & \text{otherwise} \end{cases} \quad (3)$$

The ADMM procedure iteratively minimizes the augmented Lagrangian over the variables  $W, Y_1, Y_2$  and updates the scaled dual variables  $U_1$  and  $U_2$ . The augmented Lagrangian  $\mathcal{L}$ , as a function of the optimization variables, is given by

$$\begin{aligned} \mathcal{L}(W, Y_1, Y_2) = & -\text{tr}(\Sigma Y_1) + \mathbf{I}_{\mathcal{F}}(Y_1) + \mathbf{I}_+(Y_2) + \alpha \|Y_2\|_1 \\ & + \frac{\rho}{2} (\|BW B^T - Y_1 + U_1\|_F^2 \\ & + \|BW B^T - Y_2 + U_2\|_F^2) + \text{const} \end{aligned} \quad (4)$$

where  $U = (1/\rho)Z$  are the scaled dual variables  $Z$  and  $\|\cdot\|_F$  is the Frobenius norm of a matrix. The constant represents all the terms that do not depend on the optimization variables.

The variable  $W$  at iteration  $(t+1)$  is a solution to an unconstrained least squares problem,

$$\begin{aligned} W^{(t+1)} = \arg \min & \left( \|BW B^T - Y_1^{(t)} + U_1^{(t)}\|_F^2 \right. \\ & \left. + \|BW B^T - Y_2^{(t)} + U_2^{(t)}\|_F^2 \right), \end{aligned} \quad (5)$$

which can be efficiently solved using iterative methods [4, 6]. The variable  $Y_1$  update is given by

$$\begin{aligned} Y_1^{(t+1)} = \arg \min & \left( \mathbf{I}_{\mathcal{F}}(Y_1) \right. \\ & \left. + \|Y_1 - (BW^{(t+1)} B^T + U_1^{(t)} + \Sigma/\rho)\|_F^2 \right) \\ = \mathcal{P}_{\mathcal{F}} & \left( BW^{(t+1)} B^T + U_1^{(t)} + \Sigma/\rho \right), \end{aligned} \quad (6)$$

where  $\mathcal{P}(X)$  is the Euclidean Fantope projection operator which can be efficiently computed using the following lemma [5].

**Lemma 1.1** *If  $X = \sum_i \lambda_i u_i u_i^T$  is a spectral decomposition of  $X$ , then  $\mathcal{P}_{\mathcal{F}}(X) = \sum_i \hat{\lambda}_i(\theta) u_i u_i^T$ , where  $\hat{\lambda}_i(\theta) = \min(\max(\lambda_i - \theta, 0), 1)$  and  $\theta$  satisfies the equation  $\sum_i \hat{\lambda}_i(\theta) = 1$ .*

The variable  $Y_2$  update is given by a solution to

$$\begin{aligned} Y_2^{(t+1)} &= \arg \min \left( \alpha \|Y_2\|_1 + \mathbf{I}_+(Y_2) \right. \\ &\quad \left. + \frac{\rho}{2} \|BW^{(t+1)}B^T - Y_2 - U_2^{(t)}\|_F^2 \right) \\ &= \mathcal{H}_{\alpha/\rho} \left( BW^{(t+1)}B^T + U_2^{(t)} \right) \end{aligned} \quad (7)$$

which is a LASSO problem constrained to nonnegative solutions. It is solved by applying a hinge-loss function [2]

$$\mathcal{H}_{\alpha/\rho}(x) = (|x| - \alpha/\rho)_+, \quad (8)$$

to every entry of  $BW^{(t+1)}B^T + U_2^{(t)}$ . Finally, an ADMM iteration is concluded by updating the scaled dual variables

$$\begin{aligned} U_1^{(t+1)} &= U_1^{(t)} + BW^{(t+1)}B^T - Y_1^{(t+1)} \\ U_2^{(t+1)} &= U_2^{(t)} + BW^{(t+1)}B^T - Y_2^{(t+1)}. \end{aligned} \quad (9)$$

The ADMM solution is now used to deflate the covariance matrix. The deflated covariance matrix is used to derive the next nonnegative, sparse PCA direction.

## 2. RGB camera emulation

The pixel intensity  $m_c$  produced by a surface with spectral reflectance  $r$ , illuminated with a spectral power distribution of light  $i$  and imaged through a color camera filter with transmissivity  $c$  is given by

$$m_c = \int r(\lambda) i(\lambda) c(\lambda) d\lambda. \quad (10)$$

Similarly, the pixel intensity  $m_m$  produced by the same surface, but illuminated with a different light  $x$  and observed by a monochrome camera with sensor quantum efficiency  $q$  is

$$m_m = \int r(\lambda) x(\lambda) q(\lambda) d\lambda. \quad (11)$$

In our emulation approach we are looking to find such illuminant spectral power distribution  $x$  so that pixel intensities produced by color and monochrome cameras are equal;  $m_m = m_c$ . Clearly this condition is satisfied when

$$x(\lambda) q(\lambda) = i(\lambda) c(\lambda). \quad (12)$$

If we allow  $x, q, i$  and  $c$  to represent vectorized quantities, sampled at some discrete set of wavelengths, then the illuminant  $x$  that best emulates a particular camera channel can be found by solving

$$\begin{aligned} &\text{minimize } \|\mathbf{diag}(i)c - \mathbf{diag}(q)x\| \\ &\text{subject to } x \geq 0, \end{aligned} \quad (13)$$

where  $\mathbf{diag}(x)$  distributes the vector along a diagonal of a matrix.

Sometimes, as is the case of this work, there are limitations on the light spectral power distributions that can be generated with particular hardware used. Let matrix  $B$  represent the set of basis functions that span the realizable set of illuminants, so that only illuminant spectral power distributions of the form  $x = Bw$  can be generated. The set of optimal weights  $w$  that best approximate a given color camera can be found by solving

$$\begin{aligned} &\text{minimize } \|\mathbf{diag}(i)c - \mathbf{diag}(q)Bw\| \\ &\text{subject to } Bw \geq 0. \end{aligned} \quad (14)$$

In this work the matrix  $B$  has 8 columns representing the spectral power distributions of a set of narrowband LEDs used in the experiments.

## 3. Emulated camera models

In our conventional camera emulations we used the spectral responsivity curves of 34 different cameras: AptinaMT9M031, AptinaMT9M131, Canon1DMarkIII, Canon5DMarkII, Canon20D, Canon40D, Canon50D, Canon60D, Canon300D, Canon500D, Canon600D, HasselbladH2, NikonD1, NikonD3, NikonD3X, NikonD40, NikonD50, NikonD70, NikonD80, NikonD90, NikonD100, NikonD200, NikonD200IR, NikonD300s, NikonD700, NikonD5100, NokiaN900, OlympusE-PL2, PentaxK-5, PentaxQ, PhaseOne, PtGreyGrasshopper50S5C, PtGreyGrasshopper214S5C and, SONYNEX-5N. We calibrated some of these cameras ourselves, while for the remaining ones we used the measurements of Jiang et al. [3].

## 4. Classification under broadband illumination

There is little difference in pixel classification performance of pixel measurements coming from conventional cameras and broadband illuminants. The details are shown in Fig. 1 which presents the classification performance of an average camera in the *Apples* scene. This figure is indicative of trends in *Pears* and *Lemons* scenes as well. All algorithms achieve similar performance levels across different illuminants.

In general the least performing method is Naive Bayes classification, which makes strong assumptions about conditional independence in the feature space that may not hold

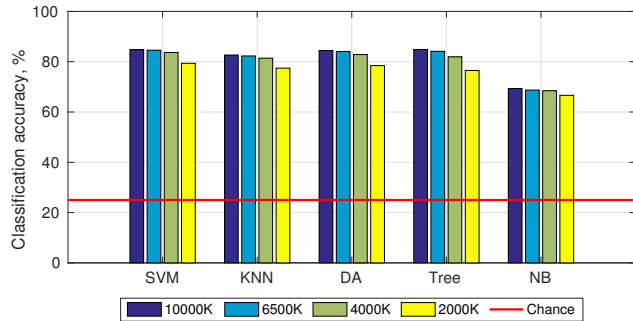


Figure 1: Pixel classification performance of conventional (RGB) cameras combined with broadband illumination (black body radiators at different temperatures). The black body radiator at 2000K and the Naive Bayes are the least performing illuminant and algorithm respectively.

true for smooth curves such as surface reflectance spectra. The black body radiator at 2000K is also consistently slightly worse for classification as it concentrates most energy at long wavelengths where reflectance spectra tend to be similar to one another.

## References

- [1] S. Boyd, N. Parikh, E. Chu, B. Peleato, and J. Eckstein. Distributed optimization and statistical learning via the alternating direction method of multipliers. *Foundations and Trends in Machine Learning*, 3(1):1–122, 2011. [1](#)
- [2] T. Hastie, R. Tibshirani, and J. Friedman. *The elements of statistical learning*. Springer, 2009. [2](#)
- [3] J. Jiang, D. Liu, J. Gu, and S. Susstrunk. What is the space of spectral sensitivity functions for digital color cameras? In *IEEE Workshop on Applications of Computer Vision, WACV*, pages 168–179, 2013. [2](#)
- [4] C. C. Paige and M. A. Saunders. Lsqqr: An algorithm for sparse linear equations and sparse least squares. *ACM Transactions on Mathematical Software*, 8(1):43–71, 1982. [1](#)
- [5] V. Vu, J. Cho, J. Lei, and K. Rohe. Fantope projection and selection: A near-optimal convex relaxation of sparse PCA. In *Advances in Neural Information Processing Systems*, pages 2670–2678, 2013. [1](#), [2](#)
- [6] S. J. Wright and J. Nocedal. *Numerical optimization*. Springer New York, 2006. [1](#)